J. Phys. B: At. Mol. Phys. **18** (1985) 125-133. Printed in Great Britain

Total electron scattering cross sections: I. He, Ne, Ar, Xe

J C Nickel†, K Imre†, D F Register‡§ and S Trajmar‡

† University of California, Riverside, CA 92521, USA

‡ Jet Propulsion Laboratory, California Institute of Technology, Pasadena, CA 91109, USA

Received 24 May 1984

Abstract. The apparatus and experimental procedures used to obtain total electron scattering cross sections are described, and results are presented for He, Ne, Ar and Xe in the 4-300 eV incident energy range, together with statistical errors. The results are generally found to be in good agreement with previous data except at low impact energies. Serious discrepancies remain in Xe below 20 eV impact energy.

1. Introduction

A large number of total electron scattering cross section (σ) measurements have been carried out in recent years for the rare gases (see table 1 for a summary for He, Ne, Ar and Xe). Most of these measurements utilised linear transmission devices. Measurements of σ obtained in this fashion are important because their accuracy depends only upon geometrical considerations of the experimental arrangement and not upon any indirect normalisation procedures. Besides their inherent importance in various modelling schemes, total cross section results serve as upper bounds for theoretical calculations, are useful inputs to the normalisation procedures used to place differential cross section measurements on an absolute scale, and are needed for checks on dispersion relations. It is important to test any new apparatus on the rare gases to assess the role of possible systematic errors and to establish a highly reliable data set for these gases. It should be noted that unresolved discrepancies still exist even in the case of the extensively studied rare gases. The present article describes the apparatus and experimental procedures used in our laboratory and presents total electron scattering cross section results for He, Ne, Ar and Xe in the 4-300 eV incident energy range.

Section 2 will describe the apparatus used to obtain the results and § 3 will outline the experimental procedure. In § 4, the present results and associated errors are summarised and compared with previously measured cross sections.

2. Apparatus

A block diagram of the linear transmission device is shown in figure 1. The construction is modular and can be considered in four sections as shown in the figure. The outer vacuum jackets of each section are constructed from non-magnetic type 321 stainless steel and the sections are joined by Varian conflat flanges, thus making the entire

§ Present address: Phillips Petroleum Co., Bartlesville, OK 74003, USA.

0022-3700/85/010125+09$02.25

Table 1. Recent total electron scattering cross section measurements on He, Ne, Ar and Xe.

Atom	Reference	Energy range (eV)	Method
Ar	Kauppila *et al* (1977)	5-15	Transmission (mag. field)
He	de Heer and Jansen (1977)	0-3000	Semiempirical
He	Blaauw *et al* (1977)	15-750	Transmission
He	Jost and Mollenkamp (1977)	150-500	RPD
He, Ne	Stein *et al* (1978)	0.25-24	Transmission (mag. field)
He	Kennerly and Bonham (1978)	1-50	TOF
Xe	Guskov *et al* (1978)	0.025-1	TOF
He	Dalba *et al* (1979)	100-1400	Modified Ramsauer type
Ne, Ar, Xe	de Heer *et al* (1979)	20-3000	Semiempirical
He	Blaauw *et al* (1980)	15-750	Transmission
He	Charlton *et al* (1980)	2-50	TOF
Ne, Ar, Xe	Wagenaar and de Heer (1980)	25-750	Transmission
Ne	O'Malley and Crompton (1980)	0-2.18	Swarm
Xe	Dababneh *et al* (1980)	0.35-100	Transmission
He, Ne, Ar	Kauppila *et al* (1981)	15-80	Transmission (mag. field)
Xe	Dababneh *et al* (1982)	20-800	Transmission
Ar, Xe	Jost *et al* (1983)	0.05-60	Transmission
Ar, Xe	Wagenaar (1984)	15-750	Transmission
He, Ne, Ar, Xe	Present	4-300	Transmission

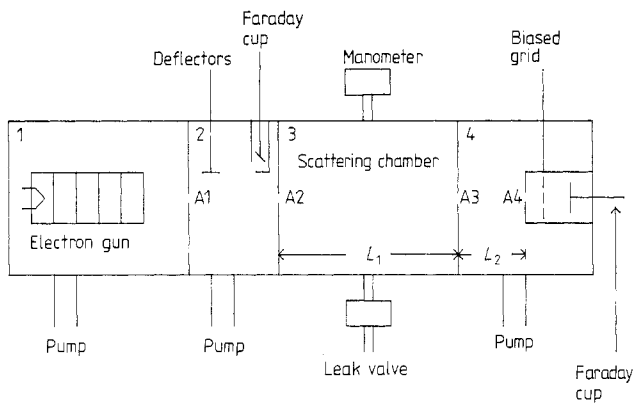

Figure 1. Schematic diagram of the apparatus.

system demountable and bakable. All apertures and deflectors are constructed from molybdenum. The entire device is enclosed in a mu-metal shield to reduce the effects of the Earth's magnetic field.

Section 1 contains a six-element, cylindrical-tube electron gun capable of generating a 5 μA beam in the selectable energy range of 4-300 eV with an energy resolution of 0.35 eV FWHM. The gun enclosure is differentially pumped to minimise such deleterious effects as filament cooling and poisoning due to gases entering the region through the 0.762 cm diameter aperture A1.

Section 2 serves three purposes. First, it acts as a differential pumping chamber to remove gas effusing from the scattering chamber. (It is important to keep the target

gas density outside the scattering chamber well below 1% of the density inside the chamber so that a well defined scattering length exists.) Second, it contains a Faraday cup, FC1, which serves to monitor the stability of the incident electron beam. Finally, section 2 contains an orthogonal set of electrostatic beam deflectors which aid in beam steering.

Section 3, the scattering chamber, is a stainless-steel tube 14.43 cm long bounded by apertures A2 and A3. Both aperture openings are 1 mm in diameter. Gas is fed to the chamber through a leak valve and the pressure in the chamber is monitored by an MKS Baratron capacitance manometer. The MKS unit consists of a model 310 BHS 1 Torr full scale sensor head and a model 170M-6C electronics unit. The temperature of the scattering chamber is monitored with a calibrated thermistor.

Section 4 again serves as a differential pumping chamber but also contains the detector, a gridded Faraday cup. The opening of the detector aperture, A4, is 2.2 mm in diameter and is located 7.1 cm from A3. The grid, when properly biased, serves to discriminate against electrons inelastically scattered in the forward direction. The output of the detector, FC2, is monitored on an electrometer.

3. Experimental procedure

In the linear transmission attenuation experiment, electrons of known energy are transmitted through the scattering chamber and are detected by the Faraday cup. It can be shown that to a good approximation the detected current, $I_d(n)$, is given by

$$I_d(n) = I_d(0) \exp(-\sigma_m n L) \tag{1}$$

where n is the target gas density in the scattering cell, L is the scattering length, and σ_m is the 'measured' total cross section. The measured cross section differs from the true cross section σ because the transmitted current detector cannot totally discriminate against electrons elastically scattered in the forward direction angles which are smaller than the access source angle of the detector. The fractional deviation between σ and σ_m is given by

$$\frac{\sigma - \sigma_m}{\sigma} = \frac{2\pi}{\sigma} \int_0^{\theta_{max}} \frac{d\sigma}{d\Omega} \sin\theta \, d\theta \simeq \frac{1}{\sigma} \left| \frac{d\sigma}{d\Omega} \right|_{\theta=0} \langle \Delta\Omega \rangle \tag{2}$$

where $|d\sigma/d\Omega|_{\theta=0}$ is the differential total scattering cross section in the forward direction (if discrimination against inelastic forward scattering is not made), $\langle \Delta\Omega \rangle$ is the solid angle subtended by the detector averaged over the length of the scattering chamber, and θ_{max} is the maximum scattering angle which can contribute to the transmitted signal. We will not distinguish between σ_m and σ for reasons discussed below. A plot of $\ln I_d(n)$ as a function of n yields a straight line whose slope is $-\sigma L$.

In our experiment, the detected current is measured as a function of pressure in the scattering cell, for a particular incident electron energy. The density in the scattering cell is derived from the pressure P (corrected for thermal transpiration as discussed below), using the ideal gas law $P = nKT$, where T is the measured temperature of the scattering cell. Using a least-squares fitting program, we obtain the best fit slope of the $\ln I_d(n)$ line and finally obtain σ. The maximum pressure used for a given incident energy is chosen such that the detected current drops to about half of its value at zero pressure. This range of pressure ensures that multiple scattering effects can be ignored.

After each run, the pressure is returned to zero and $I_d(0)$ is recorded to monitor any drifts in the incident electron beam flux. Typically drifts of a few per cent are obtained and are corrected for by assuming that the drifts occurred linearly over the period of the measurement. It was found that for incident electron beam currents above 5–10 nA, measured cross sections depended upon the incident current. All of the measurements reported here were made with the incident electron current in the 10^{-11} A range where the results are independent of the current.

The temperature of the capacitance manometer sensor head is maintained at 45 °C while the temperature of the scattering cell is typically 29–31 °C. Thus we might expect the pressure in the scattering chamber to be slightly less than the pressure indicated by the MKS unit due to thermal transpiration effects. The effects of thermal transpiration can be taken into account by the relation (Edmonds and Hobson 1965):

$$P_s = a(T_s/T_m)^{1/2} P_m \tag{3}$$

where P_s and T_s are the pressure and temperature in the scattering chamber, P_m is indicated by the MKS Baratron, T_m is the temperature of the MKS sensor, and a is a constant which depends on the geometry over which the temperature gradients occur. If the gradients occurred over an ideal aperture, we would expect $a = 1$ and for our conditions,

$$P_s = 0.976\ P_m. \tag{4}$$

Thus if we first calculated our cross sections using the thermostatted MKS readings, we would need to revise them upwards by 2.4% to take thermal transpiration effects into account, assuming the gradients take place over an ideal aperture. Several workers have noted that when the temperature gradients do not take place over an ideal aperture, $a > 1$, and its value depends on the particular geometry involved. We have determined the effects of thermal transpiration on our measurements by comparing cross sections obtained with the MKS thermostatted with those obtained with the MKS unit in thermal equilibrium with the scattering cell. We find thermal transpiration effects to be important only for He and Ne. The cross sections for He calculated using the thermostatted MKS readings (convenient for stability reasons) needed to be revised upwards by 2% to account for thermal transpiration while those for neon need to be revised upwards by 1%. No thermal transpiration correction was needed for Ar and Xe. The variation of thermal transpiration effects with atomic species is not understood but may be due to our particular experimental arrangement.

All gases used in these measurements were Matheson research grade. The purity, as stated by the supplier, was 99.999% for He, 99.999% for Ne, 99.9995% for Ar and 99.995% for Xe. No independent measurement of purity was made.

4. Results and discussion

The results of the present measurements are summarised in table 2 together with the statistical errors. To the statistical errors an estimated ±2% systematic error has to be added (see § 5 for detailed discussion). Comparisons between the present and other recent measurements are shown in figures 2 to 5. The error bars on the present measurements are ±3%, which give a measure of the combined statistical and systematic errors.

Table 2. Total electron scattering cross sections (Å^2). The numbers in parentheses refer to statistical errors (%).

Impact energy (eV)	Helium	Neon	Argon	Xenon
4	5.516 (0.3)	2.565 (5.4)	7.113 (1.8)	28.97 (1.1)
5	5.346 (0.8)	2.843 (1.2)	8.984 (1.0)	36.81 (0.4)
6	5.122 (0.0)	2.984 (0.1)	11.18 (2.5)	41.67 (0.2)
8	4.735 (0.7)	3.260 (1.0)	15.97 (2.9)	41.84 (1.0)
10	4.389 (0.3)	3.443 (0.4)	20.56 (1.6)	40.15 (0.4)
12	4.065 (0.6)	3.555 (0.8)	23.61 (1.0)	38.64 (1.7)
14	3.777 (0.6)	3.625 (0.3)	24.16 (2.2)	37.27 (2.1)
16	3.520 (0.3)	3.668 (0.9)	23.08 (0.7)	36.99 (0.4)
18	3.274 (0.3)	3.706 (0.8)	20.92 (1.0)	36.63 (0.8)
20	3.095 (0.4)	3.727 (0.6)	19.02 (1.1)	35.79 (0.9)
25	2.680 (0.2)	3.766 (0.8)	16.21 (1.2)	27.77 (2.6)
30	2.391 (0.1)	3.780 (1.0)	14.52 (2.8)	20.80 (1.6)
40	2.001 (0.5)	3.709 (0.7)	12.09 (0.9)	15.71 (0.7)
50	1.715 (0.9)	3.613 (0.9)	10.69 (0.7)	13.95 (0.1)
60	1.541 (0.0)	3.509 (1.1)	9.893 (0.5)	13.19 (0.3)
70	1.394 (0.9)	3.398 (0.1)	9.320 (0.7)	12.67 (0.6)
80	1.269 (2.0)	3.283 (0.8)	8.815 (0.5)	12.37 (0.7)
90	1.199 (0.9)	3.172 (0.6)	8.386 (0.3)	12.13 (0.1)
100	1.120 (0.6)	3.041 (0.3)	7.997 (0.5)	11.90 (1.3)
125	0.983 (0.3)	2.803 (0.3)	7.255 (0.2)	11.13 (0.4)
150	0.884 (1.1)	2.580 (0.2)	6.652 (0.2)	10.63 (0.2)
200	0.734 (1.2)	2.250 (0.6)	5.831 (0.6)	9.921 (0.5)
250	0.631 (0.7)	2.008 (0.5)	5.225 (0.2)	9.207 (0.0)
300	0.556 (0.5)	1.827 (0.7)	4.798 (0.2)	8.548 (0.5)

In the case of He (figure 2) excellent agreement is found among all measurements above a few eV impact energy. Elastic integral cross sections measured or calculated below the first inelastic threshold are equivalent to total scattering cross sections. Very good agreement exists between theoretical and experimental elastic scattering cross sections at these energies and they support the results of Kennerly and Bonham (1978).

For Ne the five sets of recent experimental total scattering cross sections (figure 3) agree with each other well within the associated error limits. Integral elastic cross sections calculated by Fon and Berrington (1981) at 5 and 10 eV are equivalent to total scattering cross sections and are in complete harmony with experiments.

The argon total scattering cross sections (figure 4) obtained in the six recent measurements agree with each other within the experimental error limits except around the peak values, in the 10 to 20 eV impact energy region, where a discrepancy of about 13% exists among the experimental results. Kauppila *et al* (1977, 1981) obtained low values, while the results of Jost *et al* (1983), Wagenaar (1984) and the present work represent the higher values. The Wagenaar (1984) measurements yielded excellent agreement with the present results down to 20 eV but their value at 15 eV falls in the middle of the 13% discrepancy range. (In the case of Ar and Xe we are discussing the data of Wagenaar (1984) which is slightly different from and supersedes the results of Wagenaar and de Heer (1980).)

For Xe (figure 5) the five recent measurements are in good agreement above 20 eV impact energies. The measuremens of Wagenaar (1984) and the present results are in

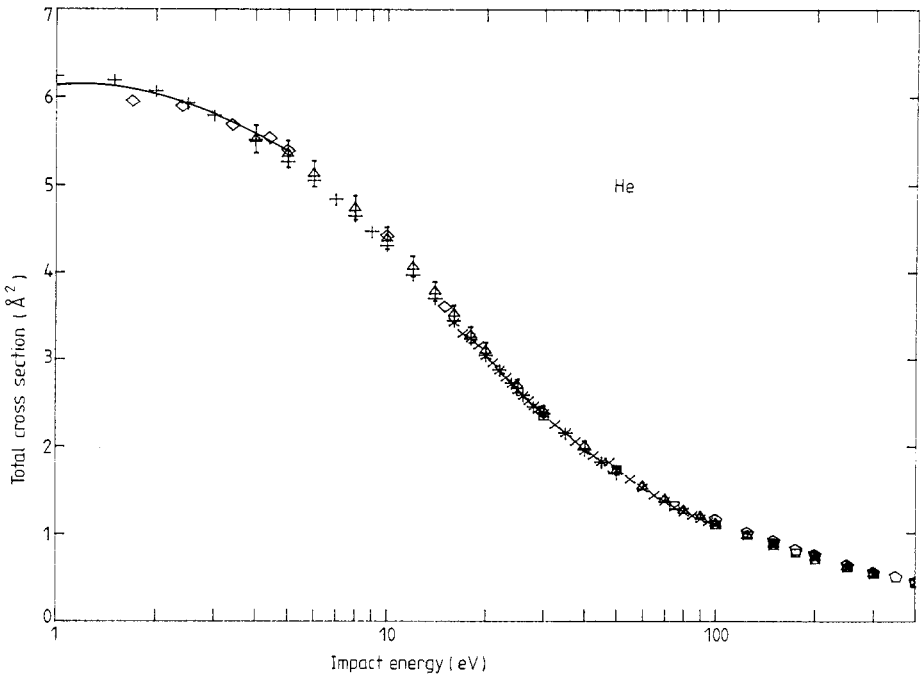

Figure 2. Total scattering cross sections for He. ○, Jost and Mollenkamp (1977); ◇, Stein *et al* (1978); +, Kennerly and Bonham (1978); ⬡, Dalba *et al* (1979); ×, Blaauw *et al* (1980); □, Kauppila *et al* (1981); ⏃, present results with error bars. The full curve in the 1 to 5 eV region represents the calculated integral elastic cross section of Nesbet (1979).

agreement within 2% over the whole energy range of overlap (20 to 300 eV). The results of Dababneh *et al* (1980, 1982) are lower by about 5 to 10% than the present results. The values obtained by Jost around 50-60 eV agree with our values within 3% but are higher than our values by about 5% between 20 and 50 eV. At lower energies there is serious disagreement. The results of Jost *et al* (1983) are considerably (nearly 20% at peak values) higher than the results of Dababneh *et al* (1980) and of the present work. Recent elastic scattering cross section calculations by McEachran and Stauffer (1984) and by Sin Fai Lam (1982) are in better agreement with the values of Jost *et al* (1983) than with the others. The reason for this discrepancy is not clear.

5. Discussion of errors

The statistical error for each point is given in table 2. Three or more (in some cases 20) measurements were made for each data point (several measurements per run and several runs). The cross section reported for each data point is the average value of all measurements. The statistical error quoted is given by

$$\% \text{ error} = \frac{1}{\sigma}\left(\sum_{i=1}^{N} \frac{(\sigma_i - \sigma)^2}{N-1}\right)^{1/2} \tag{5}$$

where σ is the average cross section, σ_i is the ith measured cross section and N is the number of measurements in the sample.

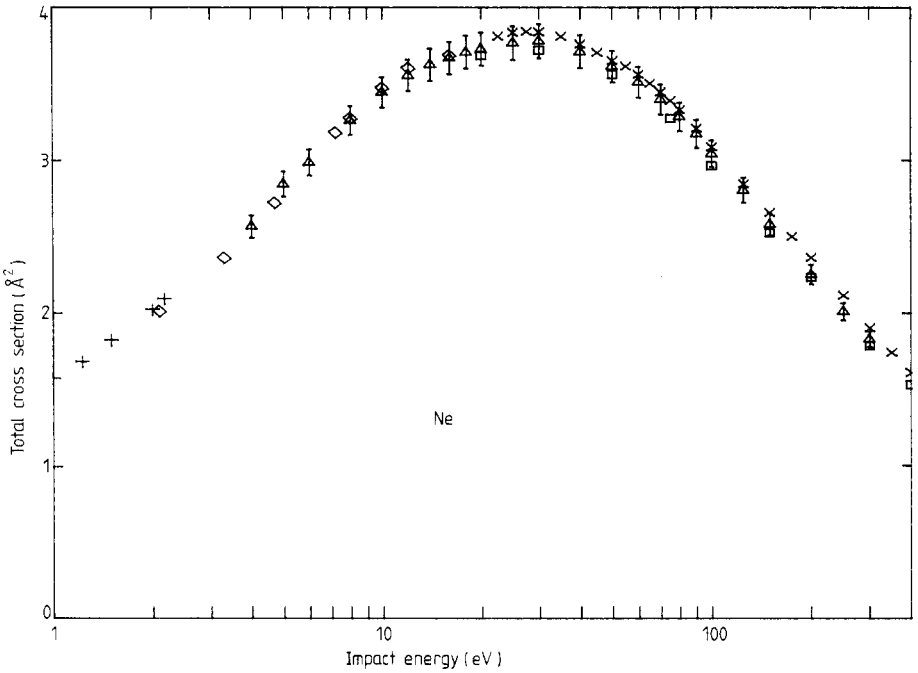

Figure 3. Total scattering cross sections for Ne. ◇, Stein *et al* (1978); ×, Wagenaar and de Heer (1980); +, O'Malley and Crompton (1980); □, Kauppila *et al* (1981); ⧫, present results with error bars.

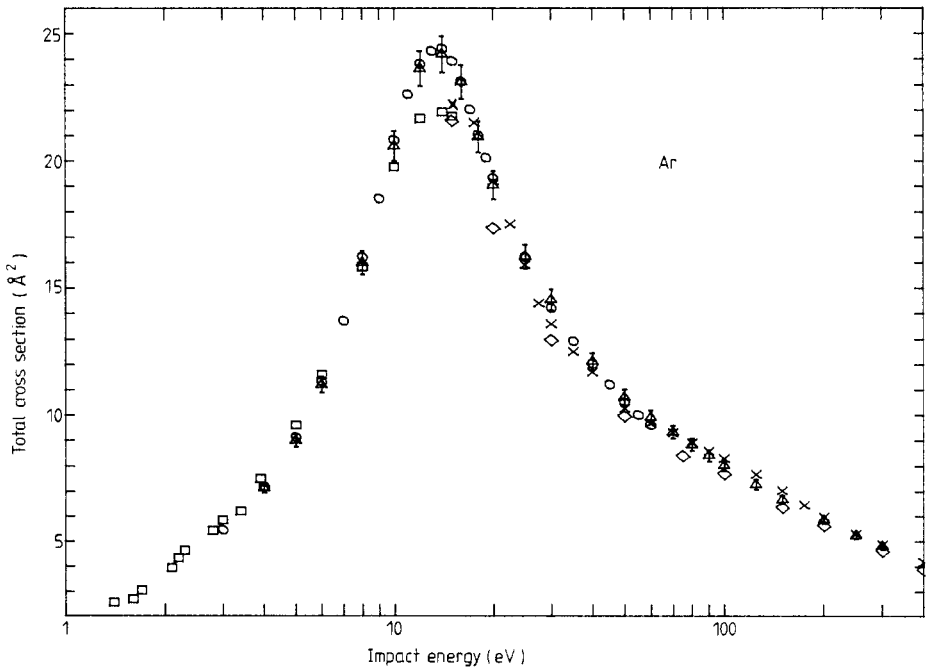

Figure 4. Total scattering cross sections for Ar. □, Kauppila *et al* (1977); ×, Wagenaar (1984); ◇, Kauppila *et al* (1981); ○, Jost *et al* (1983); ⧫, present with error bars.

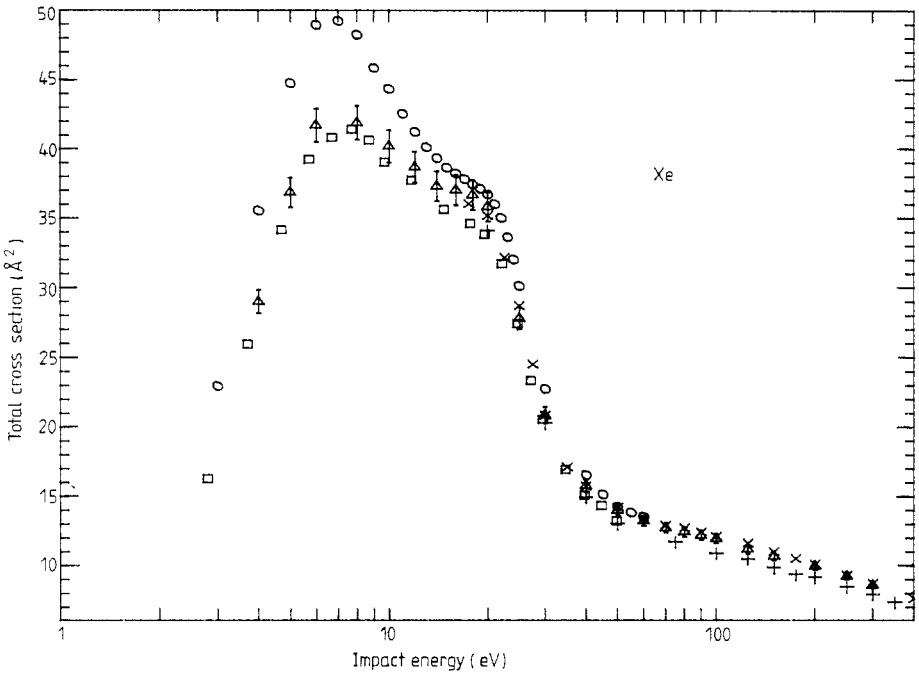

Figure 5. Total scattering cross sections for Xe. ×, Wagenaar (1984); □, Dababneh *et al* (1980); +, Dababneh *et al* (1982); ○, Jost *et al* (1983); ⊼, present results with error bars.

Four sources of systematic errors were considered.

(i) Pressure measurement. The MKS manometer is specified by the manufacturer to be accurate to better than 1% over the ranges used in these experiments. Over most of the ranges, the accuracy is specified to be much better than 1%. We assign an error of ±1% in the pressure measurement.

(ii) Effective path length L. The physical length of the scattering cell (L_2) is 14.43 cm. The electron beam must pass through the differential pumping chambers of lengths L_1 (7.0 cm) and L_3 (7.1 cm), respectively (see figure 1). Any gas in these chambers will make the effective attenuation length differ from the physical length L_2 and will tend to yield high values for the measured cross section. The error associated with effective path length considerations is given by

$$\frac{\sigma_m - \sigma}{\sigma} = \frac{\alpha(L_1 + L_3)}{L_2} \simeq \alpha$$

where α is the ratio of the density in the differential pumping chambers to the density in the scattering chamber. For our case $\alpha < 0.01$ and we assign an error of −1% to this effect.

(iii) Scattering in the forward direction. As discussed in § 2, the true cross section may differ from the measured cross section because of the contribution to the transmitted current from forward scattering. We utilised a biased grid in the Faraday cup to discriminate against electrons inelastically scattered in the forward direction. In our apparatus $\theta_{max} = 0.89°$ and $\langle \Delta\Omega \rangle = 2.2 \times 10^{-4}$ sr. Under these conditions, calculations using very-low-angle differential cross sections measured by Wagenaar (1984) show that the error introduced by forward scattering is negligible compared with other errors.

(iv) Thermal transpiration. Errors associated with thermal transpiration yield low measured cross sections in our situation. Using equation (4), we find that the maximum allowed correction in the present measurements could be 2.7%. For each measurement we corrected for thermal transpiration as discussed in § 2 and we estimate that the uncertainty generated in the cross sections by this procedure is about 1%.

Combining all systematic errors, we assign a total systematic error of ±2% to our data.

Acknowledgments

We would like to express our gratitude to R T Poe for his help in initiating this program, and our thanks to K Jost, P G F Bisling, F Eschen, M Felsmann and L Walther and to R P McEahran and A D Stauffer for making their results available to us prior to publication. This work was supported partly by University of California at Riverside Intramural Grant No 5032 and partly by the Jet Propulsion Laboratory, California Institute of Technology under contract to the National Aeronautics and Space Administration.

References

Blaauw H J, de Heer F J, Wagenaar R W and Barends D H 1977 *J. Phys. B: At. Mol. Phys.* **10** L299-303

Blaauw H J, Wagenar R W, Barends D H and de Heer F J 1980 *J. Phys. B: At. Mol. Phys.* **13** 359-76

Charlton M, Griffith T C, Heyland G R and Twomey T R 1980 *J. Phys. B: At. Mol. Phys.* **13** L239-44

Dababneh M S, Hsieh Y F, Kauppila W E, Pol V and Stein T S 1982 *Phys. Rev.* A **26** 1252-9

Dababneh M S, Kauppila W E, Downing J P, Laperriere F, Pol V, Smart J H and Stein T S 1980 *Phys. Rev.* A **22** 1872-77

Dalba G, Fornasini P, Lazzizzera I, Ranieri G and Zecca A 1979 *J. Phys. B: At. Mol. Phys.* **12** 3787-95

Edmonds T and Hobson J P 1965 *J. Vac. Sci. Technol.* **2** 182-97

Fon W C and Berrington K A 1981 *Phys. Rev.* A **14** 323-34

Guskov Y K, Savvov R V and Slobodyanynk V A 1978 *Sov. Phys.-Tech. Phys.* **23** 167-71

de Heer F J and Jansen R H J 1977 *J. Phys. B: At. Mol. Phys.* **10** 3741-58

de Heer F J, Jansen R H J and van der Kay 1979 *J. Phys. B: At. Mol. Phys.* **12** 979-1002

Jost K, Bisling P G F, Eschen F, Felsmann M and Walther L 1983 *Proc. 13th Int. Conf. on the Physics of Electronic and Atomic Collisions, Berlin* ed J Eichler *et al* (Amsterdam: North-Holland) Abstracts p 91 and private communication

Jost K and Mollenkamp R 1977 *Proc. 10th Conf. on Physics of Electronic and Atomic Collisions* (Paris: Commisariat à l'Energie Atomique) Abstracts p 395

Kauppila W E, Stein T S, Jesion G, Dababneh M S and Pol V 1977 *Rev. Sci.* **48** 822-28

Kauppila W E, Stein T S, Smart J H, Dababneh M S, Ho Y K, Downing J P and Pol V 1981 *Phys. Rev.* A **24** 725-42

Kennerly R E and Bonham R A 1978 *Phys. Rev.* A **17** 1844-54

McEachran R P and Stauffer A D 1984 *J. Phys. B: Mol. Phys.* **17** 2507-18

Nesbet R K 1979 *Phys. Rev.* A **20** 58-70

O'Malley T F and Crompton R W 1980 *J. Phys. B: At. Mol. Phys.* **13** 3451-64

Sin Fai Lam L T 1982 *J. Phys. B: At. Mol. Phys.* **15** 119-42

Stein T S, Kauppila W E, Pol V, Smart J H and Jession G 1978 *Phys. Rev.* A **17** 1600-8

Wagenaar R 1984 *Thesis* Amsterdam

Wagenaar R W and de Heer F J 1980 *J. Phys. B: At. Mol. Phys.* **13** 3855-66